FULL PAPERS

Magnetic Resonance in Medicine 61:260–266 (2009)

Selective Resonance Suppression ^{1}H-[^{13}C] NMR Spectroscopy With Asymmetric Adiabatic RF Pulses

Lijing Xin,[1] Hanne Frenkel,[1] Vladimír Mlynárik,[1] Florence D. Morgenthaler,[1] and Rolf Gruetter[1–3]*

Despite obvious improvements in spectral resolution at high magnetic field, the detection of ^{13}C labeling by ^{1}H-[^{13}C] NMR spectroscopy remains hampered by spectral overlap, such as in the spectral region of ^{1}H resonances bound to C3 of glutamate (Glu) and glutamine (Gln), and C6 of N-acetylaspartate (NAA). The aim of this study was to develop, implement, and apply a novel ^{1}H-[^{13}C] NMR spectroscopic editing scheme, dubbed "selective Resonance suppression by Adiabatic Carbon Editing and Decoupling single-voxel STimulated Echo Acquisition Mode" (RACED-STEAM). The sequence is based on the application of two asymmetric narrow-transition-band adiabatic RF inversion pulses at the resonance frequency of the ^{13}C coupled to the protons that need to be suppressed during the mixing time (TM) period, alternating the inversion band downfield and upfield from the ^{13}C resonance on odd and even scans, respectively, thus suppressing the detection of ^{1}H resonances bound to ^{13}C within the transition band of the inversion pulse. The results demonstrate the efficient suppression of ^{1}H resonances bound to C3 of Glu and Gln, and C4 of Glu, which allows the ^{1}H resonances bound to C6 of NAA and C4 of Gln to be revealed. The measured time course of the resolved labeling into NAA C6 with the new scheme was consistent with the slow turnover of NAA. Magn Reson Med 61:260–266, 2009. © 2009 Wiley-Liss, Inc.

Key words: N-acetylaspartate; asymmetric adiabatic pulse; ^{1}H-[^{13}C] NMR spectroscopy; RACED-STEAM; glutamate; in vivo

The detection of ^{13}C label incorporation in conjunction with ^{13}C-labeled substrate administration is an important strategy to study brain metabolism noninvasively. Many in vivo ^{13}C NMR spectroscopy studies have detected the label incorporation into metabolites such as glutamate (Glu) and glutamine (Gln) from ^{13}C labeled glucose or acetate in animal and human brain (1–7). Such studies have permitted the assessment of the tricarboxylic acid cycle rate (5,8,9). Similarly, ^{13}C magnetic resonance spectroscopy (MRS) has further been used to determine the metabolic rate of other neurochemicals, such as N-acetylaspartate (NAA) and glutathione, in vivo (10).

The large chemical shift dispersion of ^{13}C provides abundant spectral information; nevertheless, the low sensitivity of ^{13}C demands a larger volume in vivo (11). In contrast to direct detection by ^{13}C NMR spectroscopy, indirect detection through ^{1}H bound to ^{13}C can offer higher sensitivity and thus spatial resolution, albeit at lower spectral resolution. With increasing magnetic field strength, the progressive improvement in spectral sensitivity and resolution enhances the investigational capabilities of ^{1}H-[^{13}C] NMR spectroscopy (12–14).

Although elegant ^{1}H-[^{13}C] NMR spectroscopic approaches based on heteronuclear multiple quantum coherence (HMQC) and single quantum coherence (HSQC) editing techniques have been reported (15,16), traditionally most approaches combine three-dimensional localization with Proton Observed Carbon Edited (POCE) NMR based on inverting the magnetization of protons bound to ^{13}C on alternate spin-echo scans (17,18). The difference and sum spectra provide the resonance signals from protons bound to ^{13}C and ^{12}C, respectively. In addition, an "adiabatic carbon editing and decoupling single-voxel stimulated echo acquisition mode" (ACED-STEAM) sequence based on editing of $\pm I_z S_z$ coherences during the TM period has been developed (14).

Despite the improvements in sensitivity and spectral resolution at high magnetic field strengths, such as 9.4 T, combined with high shimming performance (19) and advanced quantitation methods (20) that allow ^{1}H-[^{13}C] NMR spectroscopy to provide abundant spectral information (14), spectral overlap remains in certain regions of interest. For instance, the observation of ^{13}C label incorporation into the acetyl group of NAA (NAA C6) at 2.01 ppm is easily obscured by the intensive labeling of Glu C3 and Gln C3 (Glx C3) at 2.04–2.13 ppm due to their complex coupling patterns and rapid labeling at the beginning of the infusion study. Likewise, Gln C4 often appears as a partially resolved shoulder of Glu C4 (12). Such overlap can lead to large standard deviations (SDs) in quantitation of these metabolites even when using a sophisticated spectral fitting program such as LCModel (20). The measurement of Gln C4 turnover is important for assessing cerebral compartmentation between neurons and glia (7,8). On the other hand, NAA is generally considered as an inert molecule with an unknown role. The recent demonstration of its active metabolism (21) suggested that the regional mea-

[1]Laboratory of Functional and Metabolic Imaging (LIFMET), École Polytechnique Fédérale de Lausanne, Lausanne, Switzerland.

[2]Department of Radiology, University of Lausanne, Lausanne, Switzerland.

[3]Department of Radiology, University of Geneva, Geneva, Switzerland.

Grant sponsor: National Institutes of Health; Grant number: R01NS042005; Grant sponsor: Swiss National Science Foundation; Grant number: SNF 3100A0-116220; Grant sponsors: Centre d'Imagerie BioMédicale (CIBM); University of Lausanne (UNIL); University of Geneva (UNIGE); Hopitaux Universitaire de Genève (HUG); Centre Hospitalier Universitaire Vaudois (CHUV); Ecole Polytechnique Fédérale de Lausanne (EPFL); Leenaards Foundation; Jeantet Foundation.

*Correspondence to: Rolf Gruetter, Ph.D., École Polytechnique Fédérale de Lausanne, SB-LIFMET, CH F0 632, Station 6, CH-1015 Lausanne, Switzerland. E-mail: rolf.gruetter@epfl.ch

Received 21 May 2008; revised 4 August 2008; accepted 2 September 2008.

DOI 10.1002/mrm.21829

Published online in Wiley InterScience (www.interscience.wiley.com).

surement of the NAA metabolism may give insight into the role of this abundant amino acid.

Therefore, the aim of the present study was threefold: 1) to develop and implement a ^1H-[^{13}C] NMR spectroscopic editing scheme, based on "selective Resonance suppression by Adiabatic Carbon Editing and Decoupling single-voxel STimulated Echo Acquisition Mode" (RACED-STEAM) using two asymmetric narrow-transition-band adiabatic RF pulses to reveal specific ^{13}C labeled ^1H resonances; 2) to validate the efficiency of the scheme in vitro and in vivo; and 3) to measure the NAA C6 turnover time course in vivo in the rat brain using the proposed scheme.

MATERIALS AND METHODS

Phantom and Animal Preparation

For pulse sequence validation a 15-ml plastic cylinder tube containing a 20 mM 99% enriched [1,2-$^{13}C_2$] sodium acetate solution (ISOTEC Inc., Miamisburg, OH, USA) was prepared.

All animal procedures were in accordance with local and federal guidelines and were approved by the local ethics committee. For in vivo validation of the proposed scheme, five healthy Sprague Dawley rats were fasted overnight, anesthetized by 2% isoflurane during the experiment and prepared as follows: one femoral vein and artery were cannulated for continuous infusion of a 20% (w/v) solution of 99% enriched [U-$^{13}C_6$] glucose (ISOTEC Inc.) and blood sampling, respectively.

NAA turnover experiments were performed on another five healthy Sprague Dawley rats (238 ± 15 g, mean ± SD) that were fasted overnight (14–16 h) with free access to water before the studies. During surgery and preparation, the animals were intubated and ventilated by 2% isoflurane. One femoral vein and artery were cannulated for continuous infusion of α-chloralose (Fisher Scientific, Pittsburgh, PA, USA) and [U-$^{13}C_6$] glucose (67% enriched; ISOTEC Inc.) and blood sampling, respectively. After the surgery, anesthesia was switched to α-chloralose, an 80-mg/kg bolus of α-chloralose was given initially and later anesthesia was maintained by continuous infusion of α-chloralose at a rate of ~26.7 mg/kg/h. The animal was placed in an in-house-built holder and the head was fixed by a bite bar and a pair of ear bars. Respiration rate and blood pressure were monitored by a small-animal monitor (SA Instruments Inc., New York, NY, USA). A 3.3-ml/kg bolus of a 20% (w/v) solution of 99% enriched [U-$^{13}C_6$] glucose was initially given over the first 5 min and a 67% enriched [U-$^{13}C_6$] glucose solution was continuously infused by a lower rate, which was adjusted to maintain the plasma glucose concentration at ~16 mM during the entire experiment. Approximately every 30 min, arterial blood was sampled to monitor the blood gases (pCO_2, pO_2), pH, and plasma glucose concentration. The respiration rate and volume were adjusted to maintain the pH and blood gases in the physiological range. Body temperature was measured by a rectal thermosensor and maintained at 38.0°C ± 0.5°C with the circulation of heated water.

Brain Extract Preparation and In Vitro NMR

After in vivo MRS measurements, the animal was killed by focused microwave irradiation within 1.4 s (4 kW, Gerling Applied Engineering, Inc., Modesto, CA, USA) and the brain was taken out and preserved in a −80°C freezer for further extract preparation. The frozen brain was crushed to fine powder under liquid nitrogen with a mortar and pestle. The brain powder was extracted with 0.9 M perchloric acid and neutralized with 9 M potassium hydroxide. The supernatant of the extract solutions was filtered with a 0.22-μm filter (Millipore Corp., Billerica, MA, USA), lyophilized, and resuspended in 100% D_2O for high-resolution NMR spectroscopy. The pH of the solution was adjusted to ~2 by deuterated perchloric acid to resolve the NAA peaks from the NAAG and Glx peaks in the high-resolution ^1H spectra. The brain extract measurements were performed on a 600-MHz vertical-bore DMX-600 spectrometer (Bruker, Fallanden, Switzerland). A 1D ^1H pulse-and-acquire sequence was used to measure the isotopic enrichment of NAA and glucose in the brain extract (TR = 15 s).

Pulse Sequence

The RACED-STEAM ^1H-[^{13}C] NMR spectroscopic editing approach was implemented based on the ACED-STEAM sequence (14) with two asymmetric narrow-transition-band adiabatic RF pulses applied in the ^{13}C channel during TM in alternate scans (Fig. 1). "VAriable RF Pulses with Optimized Relaxation delays" (VAPOR) water suppression along with three interleaved outer volume suppression modules were applied prior to the STEAM sequence (22). Low-power adiabatic ^{13}C decoupling based on an adiabatic hyperbolic secant pulse (HS8) combined with both Malcom-levitt (MLEV)-4 and a five-step phase cycling was applied during the acquisition as described previously (14).

Editing was achieved as in ACED-STEAM (14), except that two asymmetric narrow-transition-band adiabatic RF pulses with mirrored excitation profiles were applied in the ^{13}C channel in alternate scans for ^{13}C inversion. The first asymmetric narrow-transition-band adiabatic RF pulse (termed "asymmetric pulse") was formed from the first half of an HS_2^1 pulse (6000 points, $R = 0.67$) and from the second half of a tanh/tan pulse (400 points, $R = 112$) (23,24). At a $\gamma B_{1max}/2\pi$ of 1 kHz and a pulse length of 20 ms, an 83 Hz transition bandwidth ($-0.95 < M_z/M_0 < 0.95$) and 3.25 kHz inversion bandwidth ($-1 < M_z/M_0 < -0.95$) downfield from the carrier frequency was achieved. The center of the transition band ($M_z = 0$) was placed at the carrier frequency. The second pulse was created by mirroring the frequency modulation function of the first pulse, which provided a mirror profile for inversion (termed "anti-asymmetric pulse"), i.e., inversion over ~3.25 kHz upfield from the carrier frequency.

On odd scans the asymmetric pulse was applied to invert the resonances downfield, and on even scans the anti-asymmetric pulse was applied to invert upfield, yielding a ^1H-[^{13}C] NMR spectrum with opposite sign for those ^1H resonances bound to ^{13}C on opposite sides of the ^{13}C carrier frequency. This scheme allowed for suppression of ^1H resonances bound to ^{13}C nuclei resonating within the transition band of the asymmetric adiabatic pulses.

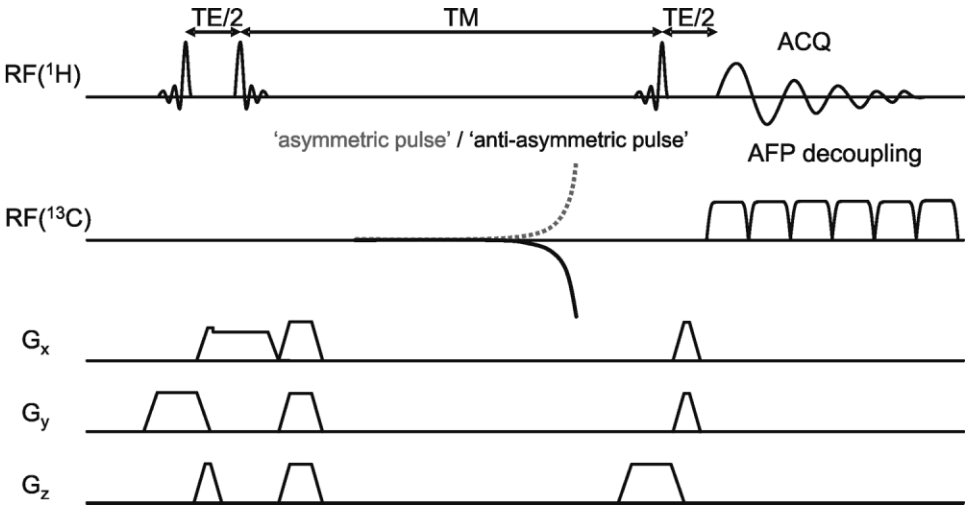

FIG. 1. Selective resonance suppression ^{1}H-[^{13}C] NMR sequence (RACED-STEAM). Two asymmetric adiabatic inversion pulses are applied in the ^{13}C channel on alternate scans, where the direction of the adiabatic sweep is alternated (indicated by the dashed line). Broadband adiabatic decoupling is applied during the acquisition.

MRS

All phantom and in vivo MRS experiments were carried out on an INOVA spectrometer (Varian, Palo Alto, CA, USA) interfaced to an actively-shielded 9.4 T/31 cm horizontal-bore magnet (Magnex Scientific, Abingdon, UK) with 12-cm inner diameter (i.d.) high-performance gradients (400 mT/m in 120 μs). An in-house-built probe (25) with a quadrature ^{1}H surface coil (14 mm diameter) and a three-turn linearly polarized ^{13}C coil (10 mm diameter) was used as a transceiver placed on the top of the animal's head. A sphere filled with 99% ^{13}C-enriched formic acid was fixed at the center of the ^{13}C coil to provide a reference signal for power calibration of the ^{13}C editing pulse. Fast automatic shimming using FAST(EST)MAP (19) based on EPI was used to adjust all first- and second-order shims, which resulted in a full-width at half-maximum of the water signal of 14–16 Hz from a volume of 75 μl in vivo.

To illustrate the effective transition bandwidth, the ^{1}H-[^{13}C] resonance suppression efficiency of applying the asymmetric pulse on ^{13}C nuclei at different transmitter frequency offsets was simulated based on density matrix formalism for CH, CH_2, and CH_3 spin systems (J_{CH} = 130 Hz and J_{CC} = 50 Hz).

For in vitro validation, the asymmetric pulse was applied at a series of ^{13}C frequency offsets relative to the C2 of sodium acetate with broadband ^{13}C decoupling during the acquisition (TE = 7.9 ms, TM = 25 ms, TR = 4 s, the pulse length of the ^{13}C editing pulse was 20 ms during all studies).

In vivo performance was evaluated using the following four acquisitions: the aforementioned asymmetric adiabatic pulses were applied at the ^{13}C resonance of Glu C4 (scan A: asymmetric pulse; scan B: anti-asymmetric pulse) and ^{13}C resonance of Glu C3 (scan C: asymmetric pulse; scan D: anti-asymmetric pulse), respectively. These four scans were acquired in an interleaved manner and stored separately in computer memory (TE = 7.9 ms, TM = 25 ms, TR = 4 s, 512 averages total and volume of interest [VOI] = 224 μl).

For in vivo NAA C6 dynamic labeling time course measurement, the proposed scheme was used by applying the two asymmetric adiabatic pulses at the ^{13}C resonance of Glu C3 (27.86 ppm) in alternate scans (26) (TE = 7.9 ms, TM = 25 ms, TR = 4 s). The ^{13}C resonance frequency of Glu C3 was calculated from the frequency of ^{1}H (water) signal based on a previous in vivo calibration. To verify the precision of the frequency of Glu C3, the frequency of Glc C1β (96.81 ppm) was measured through an unlocalized distortionless enhancement by polarization transfer (DEPT) sequence (27) following the 99% enriched [U-$^{13}C_6$] Glc bolus to derive the frequency of Glu C3 (26), and the discrepancy between the measured frequencies of Glu C3 and those calculated was below 15 Hz. All spectra were acquired in an interleaved fashion to minimize effects of instrumental drift. Each data block saved to disk contained two free induction decays (FIDs) of 64 averages each (~8.5 min). The time course of the NAA isotopic enrichment was calculated from six blocks of scans, resulting in a temporal resolution of 51 min. After B_0 correction, six FIDs edited by the asymmetric pulse and six edited by the anti-asymmetric pulse were summed separately, and then these two summed spectra were subtracted to obtain edited spectra containing only the protons bound to ^{13}C. All the spectra were acquired from a volume of 75 μl ($3 \times 5 \times 5$ mm^3) containing a mixture of cerebral cortex, corpus callosum, and hippocampus (Fig. 2).

The peak area was measured using built-in spectrometer software (VNMRJ) to calculate the ^{13}C isotopic enrichment in the present study.

RESULTS

The editing scheme showed an excellent suppression of the ^{1}H resonance bound to C2 of sodium acetate when the asymmetric pulse was applied on resonance of the sodium acetate C2 carbon (Fig. 3a). The observed transition bandwidth of ~500 Hz was larger than that of the RF pulse per se (~100 Hz), which was explained by the quartet (J_{CH} = 128 Hz) of doublet (J_{CC} = 53 Hz) resonance structure of the C2 resonance of sodium acetate covering a spectral range of ~440 Hz.

The simulated effective transition bandwidth of the asymmetric pulse for CH_3 showed a transition bandwidth identical to the in vitro result (Fig. 3b). The effective tran-

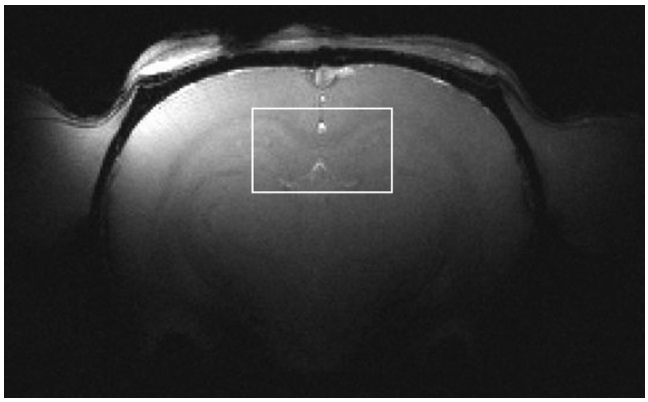

FIG. 2. Image of rat brain acquired by multislice gradient echo (TR = 150 ms, TE = 7 ms, FOV = 25 × 25 mm^2, matrix = 256 × 256, slice thickness = 1 mm) showing the VOI (3 × 5 × 5 mm^3) selected for single-voxel ^{1}H-[^{13}C] NMR measurement of NAA C6 turnover.

sition bandwidth was increased from ~250 Hz to ~500 Hz when the multiplet number was increased from CH to CH_3, consistent with the increased spread of the ^{13}C multiplets. The effective transition bandwidth of the asymmetric pulse was independent of the B_{1max} above the adiabaticity threshold (data not shown).

Spectra acquired with the proposed scheme of Fig. 1 illustrated the detection of ^{13}C label in a number of metabolites (Fig. 4). Applying the ^{13}C editing pulses on Glu C4 (subtracting scan A from B) in alternate scans suppressed the resonances of ^{1}H bound to Glu C4 and completely resolved the resonances of ^{1}H bound to Gln C4 (Fig. 4, top). The resonances downfield from the ^{13}C resonance of Glu C4 (such as Glx C2, Asp C2, tCr, and Glc C6) show negative signal intensities in the difference ^{1}H-[^{13}C] NMR spectrum, and those upfield (Gln C4, Glx C3, NAA C6, GABA C3, Lac C3, and Ala C3) show positive intensities. Note that in the same spectrum the ^{1}H resonance bound to NAA C6 at 2.01 ppm is overlapped by the more intense signal from Glx C3 at 2.04–2.13 ppm. Thus, applying the ^{13}C editing pulses at the frequency of Glu C3 (subtracting scan C from D) led to the suppression of ^{1}H resonances bound to Glx C3, thereby completely revealing the ^{1}H resonance bound to NAA C6 at 2.01 ppm (Fig. 4, bottom). Note the inverted intensity of the resonances downfield from the ^{13}C resonance of Glu C3 (such as Glx C2, Glu C4, Gln C4, Asp C2, tCr, GABA C2, and Glc C6) compared to those upfield (NAA C6, GABA C3, Lac C3, and Ala C3).

Figure 5a shows a typical ^{1}H spectrum of the rat brain featuring a high signal-to-noise ratio (SNR) and excellent spectral resolution achieved at 9.4 T. A ^{1}H-[^{13}C] NMR spectrum acquired using ACED-STEAM with a broadband adiabatic editing pulses as described previously (14) showed ^{13}C labeling in the following metabolites (dashed lines): Lac C3, Ala C3, GABA C3, Glx C3, NAA C6, Glx C4, Asp C3, tCr, GABA C2, Glx C2, Glc C6, and Asp C2 after 15 h of 67% enriched [U-$^{13}C_6$] Glc infusion. Clearly, the muliplet of Glx C3 strongly overlaps the NAA C6 signal (Fig. 5b).

With the demonstrated ability to uncover the ^{13}C-labeled NAA resonance from that of Glx C3 (Fig. 4, bottom), we sought to evaluate the metabolism of NAA. In order to assess the slow labeling of NAA C6, the suppression of Glx C3 using the proposed scheme allowed the direct observation of the ^{13}C labeling of NAA C6 (Fig. 5c). The ^{13}C downfield resonances, such as Asp C2 and C3, Glx C2 and C4, tCr, GABA C2, and Glc C6 show negative signal intensities in the ^{1}H-[^{13}C] NMR spectrum consistent with the inversion on odd scans, compared to those upfield from Glx C3, inverted on even scans (Fig. 5c). The time-resolved spectra acquired with the proposed scheme showed that the ^{13}C labeling of NAA C6 was clearly detected already within the first hour of the 67% enriched [U-$^{13}C_6$] Glc infusion despite its very slow increase (Fig. 6a).

The isotopic enrichment (IE) of NAA C6 was calculated from the following equation:

$$IE_{NAA_6} = \frac{^{13}NAA_6}{^{12}NAA_6 + {}^{13}NAA_6}. \quad [1]$$

The total NAA acetyl signal intensity was obtained by fitting the spectrum edited with the asymmetric pulse. The ^{13}C labeling signal intensity was calculated by fitting the

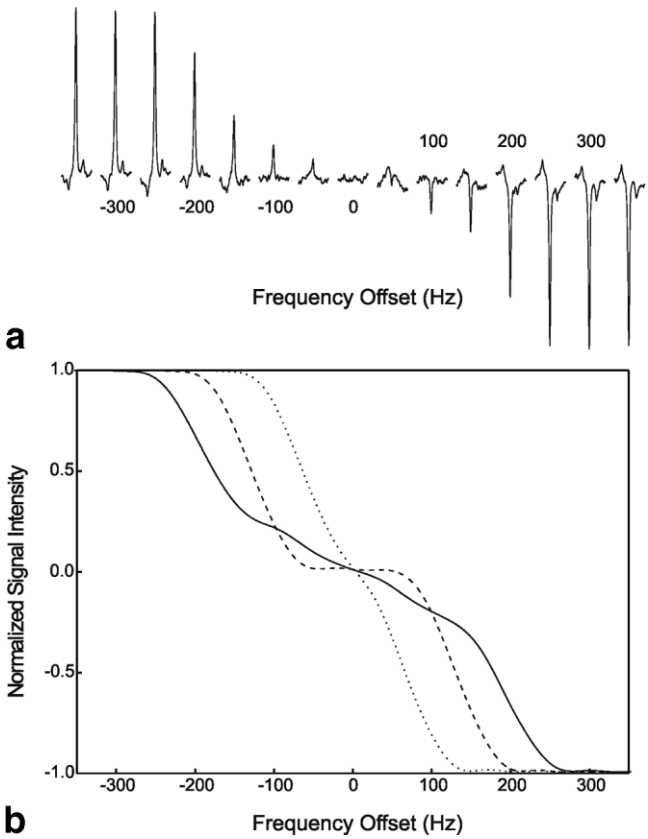

FIG. 3. ^{1}H-[^{13}C] resonance suppression efficiency. **a:** ^{1}H-[^{13}C] stack spectra (99% enriched [1, 2-$^{13}C_2$] sodium acetate) acquired with RACED-STEAM using the asymmetric pulse applied at a series of frequency offsets relative to the resonance of the C2 of sodium acetate (pulse width of asymmetric pulse was 20 ms and frequency offset increment was 50 Hz). **b:** Simulated ^{1}H-[^{13}C] resonance suppression efficiency of applying the asymmetric pulse on ^{13}C nuclei in a CH (dotted line), CH_2 (dashed line), or CH_3 spin system (solid line).

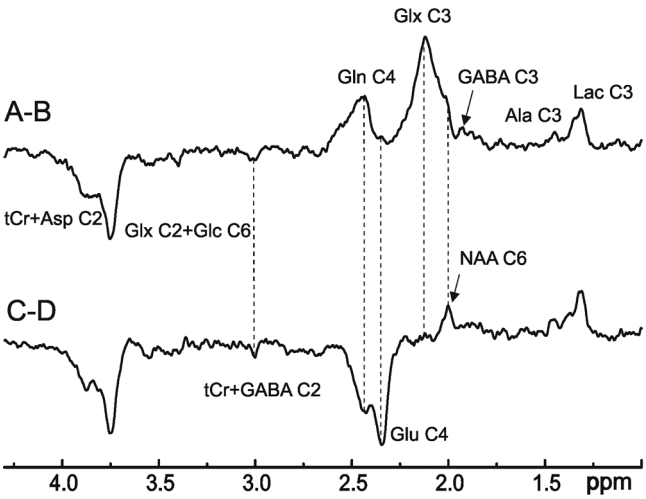

FIG. 4. ^{1}H-[^{13}C] NMR spectra obtained from a volume of 224 μl in rat brain in vivo during 99% enriched [U-$^{13}C_6$] Glc infusion. The spectra are the combination of four scans (128 averages each): (**A**) asymmetric pulse applied at the ^{13}C resonance frequency of Glu C4, (**B**) anti-asymmetric pulse applied at the ^{13}C resonance frequency of Glu C4, and (**C**,**D**) the same as (A) and (B), but with the ^{13}C editing pulses applied at the ^{13}C resonance frequency of Glu C3. In all experiments, TE = 7.9 ms, TM = 25 ms, TR = 4 s, 512 scans (~34 min), the spectra were acquired at 210–244 min from the start of the 99% enriched [U-$^{13}C_6$] Glc infusion, Gaussian function weighting = 0.15, and no baseline correction was applied.

spectrum obtained by subtracting the ^{1}H spectra edited with the asymmetric pulse and the anti-asymmetric pulse.

To validate the in vivo measurement of the NAA C6 IE, the NAA C6 IE of the last time point of each subject was compared to that measured in the brain extract and found to be in excellent agreement (slope = 0.95 ± 0.12, R^2 = 0.92, data not shown).

The time course of the NAA C6 turnover in five rats had excellent reproducibility that permitted us to overlay the individual time courses (Fig. 6b). The turnover time course of NAA C6 was fitted using the following equation (Fig. 6c):

$$\frac{^{13}\mathrm{NAA}_6(t)}{\mathrm{NAA}} = 0.67 - 0.659e^{\left(\frac{-t}{\tau_{\mathrm{NAA}_6}}\right)} \qquad [2]$$

since brain glucose IE was measured in extracts at ~67%, resulting in τ_{NAA6} = 34 ± 2.5 h (mean ± SEM, n = 5). Assuming a total [NAA] of the rat brain of 8.5 μmol/g (28), the turnover rate of NAA C6 was calculated to be 0.25 ± 0.02 μmol/g/h.

DISCUSSION

Despite the high sensitivity and excellent spectral resolution of ^{1}H-[^{13}C] NMR spectra achieved at high magnetic field combined with an efficient shimming scheme, spectral regions such as Glx C3 and NAA C6, Glu C4, and Gln C4 still have limited spectral dispersion (Fig. 5b). The current study demonstrates the potential of uncovering ^{1}H resonances bound to ^{13}C by applying asymmetric narrow-transition-band adiabatic RF pulses at the frequency of the ^{13}C chemical shift of the resonance to be suppressed. The efficiency of the scheme of Fig. 1 was verified in vivo by suppressing the overlapping resonances of Glu C4 and Glx C3 within the noise level and by resolving the ^{13}C labeled resonances of Gln C4 and NAA C6 (Fig. 4). The resolved detection of NAA C6 made it feasible to measure the time-resolved label incorporation into the NAA methyl moiety for studying NAA metabolism.

The shortest TE of ^{1}H-[^{13}C] NMR spectroscopy at which optimal editing efficiency can be achieved is $1/J_{CH}$ (~7.9 ms), which makes it difficult to implement such long narrow-transition-band adiabatic pulses with POCE-based approaches. The present scheme based on the STEAM sequence allowed to apply long editing pulses with TE = $1/J_{CH}$ and the gain of the higher spectral dispersion may thus in part offset the sensitivity disadvantage of STEAM.

Although the intrinsic transition bandwidth of the asymmetric pulse used was ~100 Hz, the effective one was broadened to ~250 Hz for CH and up to ~500 Hz for the CH_3 spin system due to J_{CC} and J_{CH} (Fig. 3b). Provided that ^{13}C resonances multiplets are separated by half of the effective transition band, this should allow the suppression of the resonance of interest without affecting nearby resonances. For instance, when the asymmetric pulses are applied on Glu C3 (CH_2), the effective transition bandwidth will be slighly larger than 380 Hz due to additional ^{13}C-^{13}C couplings. Since the ^{13}C frequency gap between Glx C3 and NAA C6 is over 400 Hz at 9.4 T, the efficient suppression of Glx C3 can be accomplished without affecting the NAA signal.

The setting of the carrier frequency of the asymmetric adiabatic pulses was continuously verified to ensure the

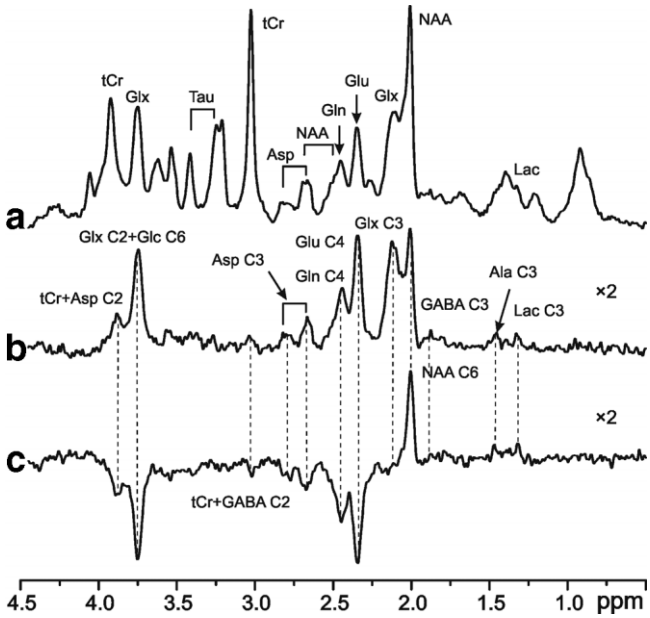

FIG. 5. Edited NMR spectra acquired using ACED-STEAM and RACED-STEAM in an interleaved manner (VOI = 75 μl, TE = 7.9 ms, TM = 25 ms, TR = 4 s, nt = 1536 total, ~102 min, 15 h after the start of 67% enriched [U-$^{13}C_6$] Glc infusion). **a:** ^{1}H spectrum of the rat brain in vivo at 9.4 T. **b:** ^{1}H-[^{13}C] spectrum using ACED-STEAM. **c:** ^{1}H-[^{13}C] spectrum of proposed RACED-STEAM scheme from the same volume with ^{13}C editing pulses applied at the ^{13}C frequency of Glu C3.

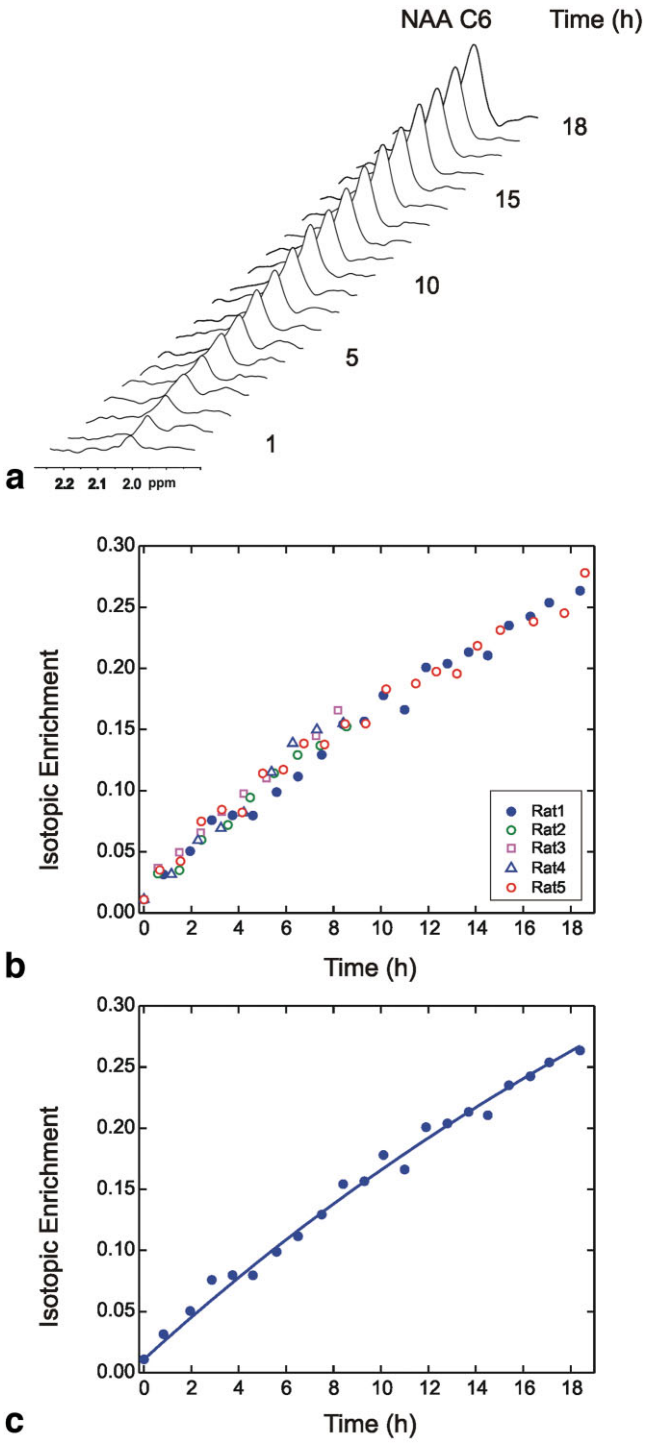

FIG. 6. NAA turnover measurements. **a:** Stack plot showing the time-resolved observation of ^{13}C incorporation into the NAA methyl resonance (NAA C6) at 2.01 ppm. Each spectrum represents 768 averages (~51 min). **b:** Time course of NAA C6 from five rats (three rats were infused by 67% enriched [U-$^{13}C_6$] Glc for 9 h, and two rats were infused for 19 h) represented by the different symbols. **c:** Fitting of the turnover in one rat using Eq. [2].

efficiency of the resonance suppression. The ^{1}H signal of a CH, CH_2, or CH_3 group was suppressed below 10% of its total intensity when the pulse offset was within the 30 Hz, 160 Hz, and 100 Hz range, respectively, around the resonance frequency of the ^{13}C signal (Fig. 3b), which is easily met under typical experimental conditions. Throughout the experiment, the ^{13}C frequency calculated from the ^{1}H resonance frequency of water had negligible discrepancy with that measured in vivo. By monitoring the frequency offset and adjusting it if necessary, an efficient suppression of ^{1}H resonances bound to ^{13}C in the in vivo spectra even in the presence of small B_0 fluctuations was ensured (Fig. 5c). Likewise, given that the ^{13}C chemical shift of Gln C3 is 0.66 ppm (66 Hz at 9.4T) upfield from Glu C3, applying editing pulses at the resonance frequency of Glu C3 also resulted in negligible residual signals of protons bound to Gln C3, especially when considering the several-fold lower concentration of Gln (28).

The inversion bandwidth of the asymmetric adiabatic pulses typically covered ~32 ppm in the ^{13}C spectrum. In the present study, the carrier frequency of the pulses was applied at the resonance of Glu C3 or Glu C4; therefore, Glc C1 was not inverted and thus not detected in the edited spectrum. The asymmetric adiabatic pulse can be modified to have a broader inversion bandwidth to cover larger ^{13}C resonances range by extending, e.g., the adiabatic sweep, which should permit the measurement of ^{13}C label in glucose to be included.

^{13}C label was detected in NAA C6 within the first hour of infusion; it increased nearly linearly with time and did not reach steady state even after 19 h (Fig. 6). The achieved complete separation of NAA C6 allowed its quantification by simple peak fitting. The isotopic enrichment was obtained directly from the edited spectra in vivo and was in excellent agreement with that measured in brain extract, thereby validating the editing scheme.

The calculated NAA C6 turnover rate of 0.25 ± 0.02 μmol/g/h was comparable to that in previously published studies (21,29–31). The lower rate and enrichment observed in this study compared to the study by Choi and Gruetter (21) may be explained by the more localized measurement of NAA turnover in the present study, and thus may imply regional differences in the NAA metabolism, e.g., a relatively higher white matter content in the current VOI (Fig. 2). The current approach can be combined with chemical shift imaging to achieve the mapping of NAA metabolism, which may provide insight into the role of this abundant amino acid.

Although the scheme of Fig. 1 was demonstrated for the detection of NAA labeling, the results also show that the Gln C4 signal can be completely separated from the strong Glu C4 resonance signal (Fig. 4, top). Since the precision of deconvolution methods critically depends on the degree of spectral overlap, the current approach is expected to significantly improve the precision of the measurement of ^{13}C labeling of Gln in ^{1}H-[^{13}C] NMR spectra, regardless of the fitting approach used. The resolved labeling of Gln C4 combined with labeling of Glu C4 should improve the ability to measure the rate of glutamatergic neurotransmitter cycle and study neuro-glial compartmentation in vivo. The labeling of GABA C3 and C2, Lac C3, Ala C3, Asp C3, Glx C2, and Asp C2 was also observed in the edited spectrum, and it potentially provides additional information for metabolic modeling.

At lower magnetic field strength, such as clinical systems at 3T, the resolved detection of Glu C3 and Glu C4 is

challenging, and approaches such as semiselective POCE NMR spectroscopy for separation of Glu C4 and Glu C3 have been suggested (32). The proposed scheme can also be extended to lower magnetic fields provided that the ^{13}C chemical shifts are sufficiently resolved, but the ^{1}H resonances strongly overlapped.

CONCLUSIONS

We conclude that the current approach provides a simple scheme for the selective suppression of ^{1}H resonances bound to ^{13}C, and allow one to uncover resonances that are difficult to resolve in the ^{1}H-[^{13}C] NMR spectrum, such as Gln C4 and NAA C6 at 9.4 T. We further conclude that NAA C6 turnover can be measured at very low levels of NAA enrichment in a small volume to study NAA metabolism in a specific cerebral region within a time frame of a few hours. The proposed scheme could also be extended to lower magnetic fields provided that the ^{13}C chemical shift remains sufficiently resolved.

ACKNOWLEDGMENT

We thank Dr. Giulio Gambarota for providing suggestions on the manuscript.

REFERENCES

1. Bluml S, Moreno A, Hwang JH, Ross BD. 1-(13)C glucose magnetic resonance spectroscopy of pediatric and adult brain disorders. NMR Biomed 2001;14:19–32.
2. Gruetter R, Novotny EJ, Boulware SD, Mason GF, Rothman DL, Shulman GI, Prichard JW, Shulman RG. Localized C-13 NMR-spectroscopy in the human brain of amino-acid labeling from D-[1-C-13]glucose. J Neurochem 1994;63:1377–1385.
3. Gruetter R, Ugurbil K, Seaquist ER. Steady-state cerebral glucose concentrations and transport in the human brain. J Neurochem 1998;70: 397–408.
4. Lebon V, Petersen KF, Cline GW, Shen J, Mason GF, Dufour S, Behar KL, Shulman GI, Rothman DL. Astroglial contribution to brain energy metabolism in humans revealed by 13C nuclear magnetic resonance spectroscopy: elucidation of the dominant pathway for neurotransmitter glutamate repletion and measurement of astrocytic oxidative metabolism. J Neurosci 2002;22:1523–1531.
5. Mason GF, Rothman DL, Behar KL, Shulman RG. NMR determination of the TCA cycle rate and alpha-ketoglutarate glutamate exchange-rate in rat-brain. J Cereb Blood Flow Metab 1992;12:434–447.
6. Rothman DL, Novotny EJ, Shulman GI, Howseman AM, Petroff OAC, Mason G, Nixon T, Hanstock CC, Prichard JW, Shulman RG. H-1[C-13] NMR measurements of [4-C-13]glutamate turnover in human brain. Proc Natl Acad Sci USA 1992;89:9603–9606.
7. Sibson NR, Shen J, Mason GF, Rothman DL, Behar KL, Shulman RG. Functional energy metabolism: in vivo C-13-NMR spectroscopy evidence for coupling of cerebral glucose consumption and glutamatergic neuronal activity. Dev Neurosci 1998;20:321–330.
8. Gruetter R, Seaquist ER, Ugurbil K. A mathematical model of compartmentalized neurotransmitter metabolism in the human brain. Am J Physiol Endocrinol Metab 2001;281:E100–E112.
9. Mason GF, Gruetter R, Rothman DL, Behar KL, Shulman RG, Novotny EJ. Simultaneous determination of the rates of the TCA cycle, glucose-utilization, alpha-ketoglutarate glutamate exchange, and glutamine synthesis in human brain by NMR. J Cereb Blood Flow Metab 1995;15: 12–25.
10. Choi IY, Gruetter R. Dynamic or inert metabolism? Turnover of N-acetyl aspartate and glutathione from D-[1-C-13]glucose in the rat brain in vivo. J Neurochem 2004;91:778–787.
11. Henry PG, Tkac I, Gruetter R. H-1-localized broadband C-13 NMR spectroscopy of the rat brain in vivo at 9.4 T. Magn Reson Med 2003; 50:684–692.
12. de Graaf RA, Brown PB, Mason GF, Rothman DL, Behar KL. Detection of [1,6-C-13]-glucose metabolism in rat brain by in vivo H-1[C-13]-NMR spectroscopy. Magn Reson Med 2003;49:37–46.
13. de Graaf RA, Mason GF, Patel AB, Behar KL, Rothman DL. In vivo 1H-[13C]-NMR spectroscopy of cerebral metabolism. NMR Biomed 2003;16:339–357.
14. Pfeuffer J, Tkac I, Choi IY, Merkle H, Ugurbil K, Garwood M, Gruetter R. Localized in vivo 1H NMR detection of neurotransmitter labeling in rat brain during infusion of [1-13C] D-glucose. Magn Reson Med 1999; 41:1077–1083.
15. van Zijl PC, Chesnick AS, DesPres D, Moonen CT, Ruiz-Cabello J, van Gelderen P. In vivo proton spectroscopy and spectroscopic imaging of [1-13C]-glucose and its metabolic products. Magn Reson Med 1993;30: 544–551.
16. Watanabe H, Ishihara Y, Okamoto K, Oshio K, Kanamatsu T, Tsukada Y. 3D localized H-1-C-13 heteronuclear single-quantum coherence correlation spectroscopy in vivo. Magn Reson Med 2000;43:200–210.
17. Fitzpatrick SM, Hetherington HP, Behar KL, Shulman RG. The flux from glucose to glutamate in the rat-brain invivo as determined by H-1-observed, C-13-edited NMR-spectroscopy. J Cereb Blood Flow Metab 1990;10:170–179.
18. Rothman DL, Behar KL, Hetherington HP, Denhollander JA, Bendall MR, Petroff OAC, Shulman RG. H-1-observe C-13-decouple spectroscopic measurements of lactate and glutamate in the rat-brain invivo. Proc Natl Acad Sci USA 1985;82:1633–1637.
19. Gruetter R, Tkac I. Field mapping without reference scan using asymmetric echo-planar techniques. Magn Reson Med 2000;43:319–323.
20. Provencher SW. Estimation of metabolite concentrations from localized in vivo proton NMR spectra. Magn Reson Med 1993;30:672–679.
21. Choi IY, Gruetter R. Dynamic or inert metabolism? Turnover of N-acetyl aspartate and glutathione from D-[1-13C]glucose in the rat brain in vivo. J Neurochem 2004;91:778–787.
22. Tkac I, Starcuk Z, Choi IY, Gruetter R. In vivo 1H NMR spectroscopy of rat brain at 1 ms echo time. Magn Reson Med 1999;41:649–656.
23. Hwang TL, van Zijl PC, Garwood M. Asymmetric adiabatic pulses for NH selection. J Magn Reson 1999;138:173–177.
24. Tannus A, Garwood M. Adiabatic pulses. NMR Biomed 1997;10:423–434.
25. Adriany G, Gruetter R. A half-volume coil for efficient proton decoupling in humans at 4 Tesla. J Magn Reson 1997;125:178–184.
26. Henry PG, Oz G, Provencher S, Gruetter R. Toward dynamic isotopomer analysis in the rat brain in vivo: automatic quantitation of 13C NMR spectra using LCModel. NMR Biomed 2003;16:400–412.
27. Henry PG, Tkac I, Gruetter R. 1H-localized broadband 13C NMR spectroscopy of the rat brain in vivo at 9.4 T. Magn Reson Med 2003;50: 684–692.
28. Pfeuffer J, Tkac I, Provencher SW, Gruetter R. Toward an in vivo neurochemical profile: quantification of 18 metabolites in short-echo-time H NMR spectra of the rat brain. J Magn Reson 1999;141:104–120.
29. Clark JB. N-acetyl aspartate: a marker for neuronal loss or mitochondrial dysfunction. Dev Neurosci 1998;20:271–276.
30. Moreno A, Ross BD, Bluml S. Direct determination of the N-acetyl-L-aspartate synthesis rate in the human brain by (13)C MRS and [1-(13)C]glucose infusion. J Neurochem 2001;77:347–350.
31. Tyson RL, Sutherland GR. Labeling of N-acetylaspartate and N-acetylaspartylglutamate in rat neocortex, hippocampus and cerebellum from [1-13C]glucose. Neurosci Lett 1998;251:181–184.
32. Henry PG, Roussel R, Vaufrey F, Dautry C, Bloch G. Semiselective POCE NMR spectroscopy. Magn Reson Med 2000;44:395–400.